ELSEVIER

Journal of Alloys and Compounds 300–301 (2000) 65–70

Journal of ALLOYS AND COMPOUNDS

www.elsevier.com/locate/jallcom

Avalanche up-conversion processes in Pr, Yb-doped materials

S. Kück*, A. Diening, E. Heumann, E. Mix, T. Sandrock, K. Sebald, G. Huber

Institut für Laser-Physik, Universität Hamburg, Jungiusstraße 9a, 20355 Hamburg, Germany

Abstract

The general characteristics of the 'photon-avalanche' up-conversion process are presented. The Pr,Yb system was spectroscopically investigated in Pr;Yb:$YLiF_4$ and Pr,Yb:$YAlO_3$ with respect to the realization and understanding of this process. Whereas Pr;Yb:$YLiF_4$ exhibits an avalanche-type excitation mechanism under infrared pumping, no such behavior is observed for Pr,Yb:$YAlO_3$. A time dependent rate equation model was developed to describe these different behaviors using experimentally determined parameters. The absence of an avalanche-type excitation mechanism in Pr,Yb:$YAlO_3$ is mainly caused by (i) a better spectral overlap between the excited state absorption in the Pr and the ground state absorption of Yb, (ii) higher transfer rates between Yb and Pr and within the Pr, and (iii) lower intrinsic decay rates from the participating excited energy levels ($^3P_{0,1,2}$ and $^1G_4$).

Keywords: Insulator; Optical properties; Luminescence

1. Introduction

Pr^{3+} exhibits a variety of laser transitions in the visible from the $^3P_{j=0,1,2}$ level [1,2] suitable for applications in display technology and medicine. Direct pumping into the $^3P_{j=0,1,2}$ levels is possible with an argon ion laser [3]. However, the overall efficiency is rather low and not interesting for application. Therefore we investigate different ways to realize laser emission from the $^3P_{j=0,1,2}$ levels by other pump sources, i.e. for example by a frequency doubled Nd-ground state laser [4]. Another way is to use infrared pump sources like laser diodes in combination with intra- and interionic energy transfer processes ('up-conversion processes'). In this contribution we discuss two possible ways, i.e. the 'photon avalanche-process' and the 'two-step absorption'. Detailed descriptions of upconversion laser processes and photon avalanche upconversion are given in [5–8]. In Pr,Yb:$YLiF_4$ (YLF) and Pr,Yb:ZBLAN fibers laser oscillation on the $Pr^{3+}(^3P_0) \rightarrow Pr^{3+}(^3F_2)$ transition via infrared pumping and 'photon avalanche' excitation was realized. On the other hand, in Pr,Yb:$YAlO_3$ a two step excitation mechanism is observed and no laser oscillation could be realized, although Pr:$YAlO_3$ exhibits efficient laser operation when directly pumped into the ^3P_j levels. The efficiency of the avalanche process strongly depends on the transfer rates between the ions, the excited state absorption cross section, the concentrations of the ions, and the radiative and total lifetimes of the participating energy levels (mainly the ^3P_j upper laser level and the $^1G_4$ intermediate storage level of Pr^{3+}).

2. Up-conversion processes and 'Photon Avalanche'

The avalanche process is a combination of several energy transfer processes and a special case of an up-conversion process. The characteristics of an 'photon-avalanche'-type process are the following: (i) The pump light is resonant to an excited state absorption (ESA) transition, but not to any ground state absorption. (ii) A critical pump power exists. Only by reaching a pump threshold value the up-conversion process is observed by detecting a considerable intense fluorescence. (iii) There is a delay between the onset of pump power and the maximum of fluorescence. This delay decreases with increasing pump power. (iv) For pump powers lower than the threshold pump power, the transmission is high (no ground state absorption). For pump powers higher than the threshold pump power, the transmission decreases. For Pr,Yb:YLF and Pr,Yb:ZBLAN fibers these characteristics are fulfilled and the following-avalanche-type-excitation scheme seems to be most favorable [1,9], see Fig. 1:

*Corresponding author. Tel.: +49-40-42838-5256; fax: +49-40-42838-6281.

E-mail address: kueck@physnet.uni-hamburg.de (S. Kück)

0925-8388/00/$ – see front matter
PII: S0925-8388(99)00734-3

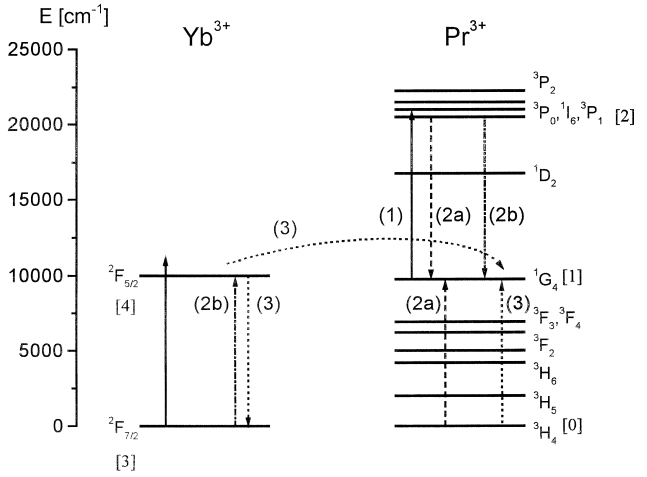

Fig. 1. Excitation scheme for the Yb–Pr avalanche pumping process. (*i*) denotes the process, [*j*] denotes the energy level used in the rate equation model (see text for further details).

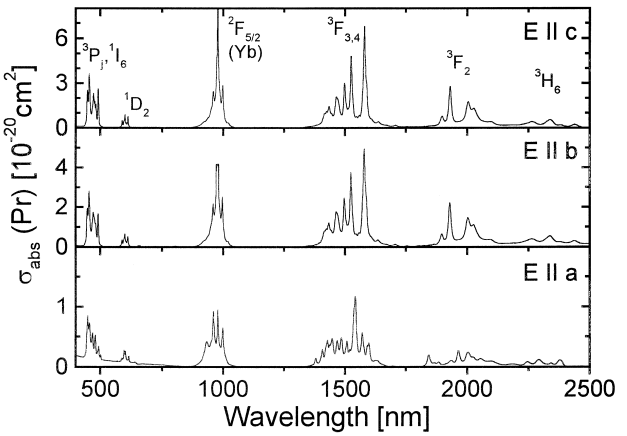

Fig. 2. Absorption spectrum of Pr,Yb:$YAlO_3$ in the three polarizations. Note that the Yb absorption is not scaled with respect to cross-sections.

(1) Excited state absorption: $Pr(^1G_4) \rightarrow Pr(^3P_{j,\ j=0,1,2}, {}^1I_6)$

(2a) Cross relaxation within the Pr: $Pr(^3P_{j,\ j=0,1,2}, {}^1I_6) + Pr(^3H_4) \rightarrow 2\ Pr(^1G_4)$

(2b) Energy transfer from Pr to Yb: $Pr(^3P_{j,\ j=0,1,2}, {}^1I_6) + Yb(^2F_{7/2}) \rightarrow Pr(^1G_4) + Yb(^2F_{5/2})$

(3) Energy transfer from Yb to Pr: $Yb(^2F_{5/2}) + Pr(^3H_4) \rightarrow Yb(^2F_{7/2}) + Pr(^1G_4)$

For up-conversion lasers, there are several demands for the host material. These are in specific a high optical quality, low phonon energies, good thermal and mechanical properties, and the realization of laser oscillation by direct pumping. In general, these demands are also fulfilled by $YAlO_3$, however, the photon avalanche process was not realized thus far.

3. Spectroscopic results

In Fig. 2 the absorption spectrum of Pr,Yb:$YAlO_3$ and in Fig. 3 the emission cross-section spectra of Pr,Yb:$YLiF_4$ and Pr,Yb:$YAlO_3$ are shown for overview. In general the emission cross-sections of Pr^{3+}:YLF are higher, especially for the $^3P_0 \rightarrow {}^3H_6$, $^3P_0 \rightarrow {}^3F_2$, and $^3P_0 \rightarrow {}^3F_4$ transitions. Furthermore the Pr^{3+} emission peaks are shifted to longer wavelengths by about 20 nm in $YAlO_3$. In Fig. 4 the excitation spectra of the red emission ($^3P_0 \rightarrow {}^3H_6$) are shown. For Pr,Yb:YLF strongest emission is observed under intense excitation in the region of the ESA bands, while for Pr,Yb:$YAlO_3$ strongest emission is observed in the spectral region of highest overlap between Yb ground state absorption and Pr excited state absorption. As a consequence, no avalanche-like excitation scheme was realized in $YAlO_3$ (compare Fig. 1 and the following discussion).

Fig. 5 depicts the temporal behavior of the Pr-emission in Yb-codoped YLF and $YAlO_3$ under infrared pumping at 854 nm. The avalanche-type behavior of Pr,Yb:YLF in contrast to Pr,Yb:$YAlO_3$ is clearly observed: For Pr,Yb:YLF a pump intensity dependent delay, typical for avalanche, between the onset of the pump pulse and the maximum of the emission intensity is observed; whereas for Pr,Yb:$YAlO_3$ the emission intensity reaches the maximum due to a two step excitation process via Yb ground state and Pr excited state absorption within interionic transfer times.

In Fig. 6a, the experimental pump power dependence of the ‘red’ emission under infrared pumping at 836 nm is shown for Pr,Yb:YLF. Both the fluorescence as well as the pump power was measured with an uncalibrated Si-detector. The measurement was performed at room temperature. The threshold-like behavior is clearly observed. In contrary, no such behavior was observed for Pr,Yb:$YAlO_3$.

The lifetimes of the ^3P_j and $^1G_4$ manifold of various Pr,Yb-doped YLF and $YAlO_3$ crystals were measured in order to determine the parameters needed in the rate equation model. The intrinsic lifetimes – i.e. the room temperature lifetimes measured in low doped samples – in YLF are 50 μs and 11 μs for the Pr ^3P_j and $^1G_4$ levels, respectively, and 2 ms for the Yb $^2F_{5/2}$ level. In $YAlO_3$ they are 12 μs and 4 μs for the Pr ^3P_j and $^1G_4$ levels, respectively, and 0,65 ms for the Yb $^2F_{5/2}$ level. The transfer parameters used in the following rate equation model were determined by measuring the concentration dependence of the relevant lifetimes.

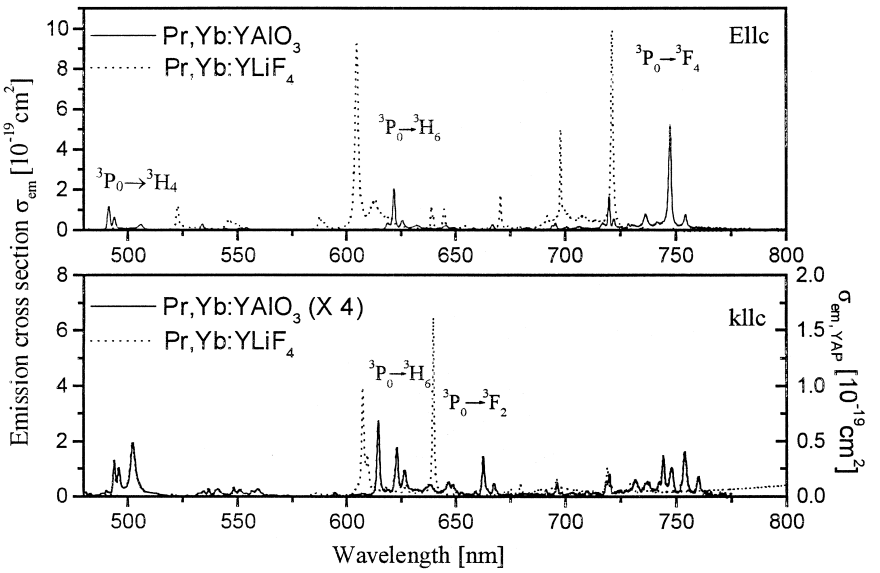

Fig. 3. Emission cross-section spectra of Pr,Yb:$YAlO_3$ and Pr,Yb:YLF.

4. Rate equation model

In the following we discuss the different behavior of Pr,Yb:YLF and Pr,Yb:$YAlO_3$ under infrared pumping with the help of a rate equation model, corresponding to the model shown in Fig. 1:

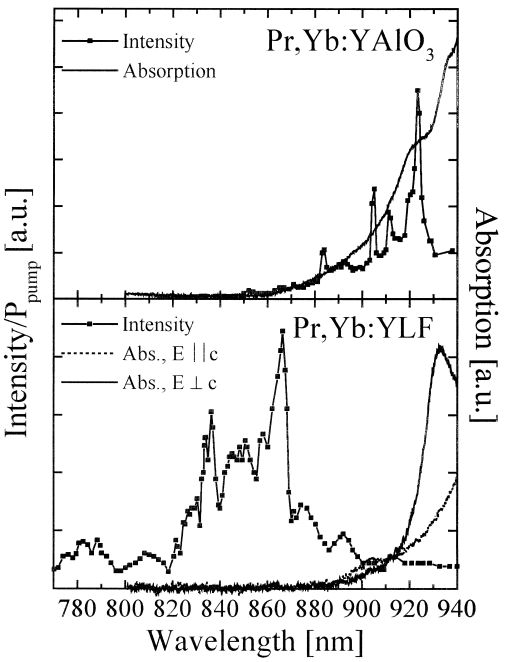

Fig. 4. Excitation spectra of the Pr^{3+} ($^3P_0$)→Pr^{3+} ($^3F_2$) transition for Pr,Yb:$YAlO_3$ and Pr,Yb:YLF in comparison to absorption.

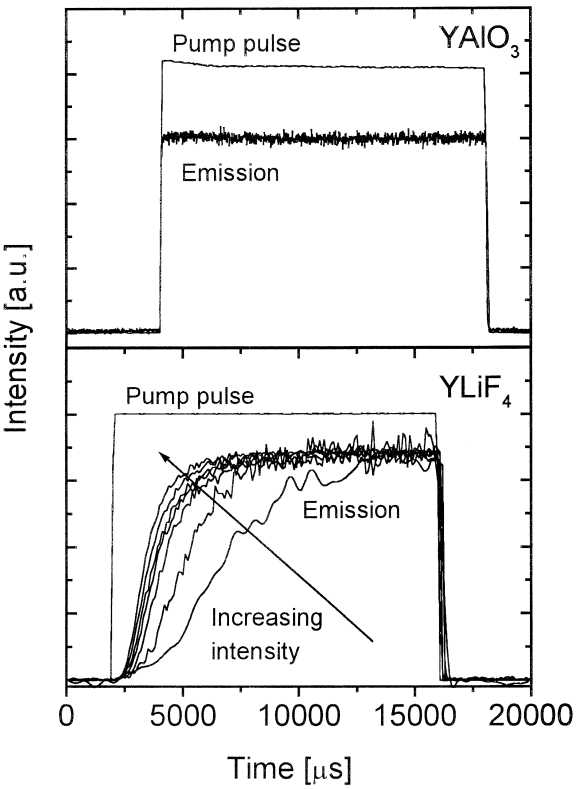

Fig. 5. Temporal behavior of Pr^{3+} ($^3P_0$)→Pr^{3+} ($^3F_2$) emission in Pr,Yb:$YAlO_3$ and Pr,Yb:YLF under quasi continuous wave infrared pumping.

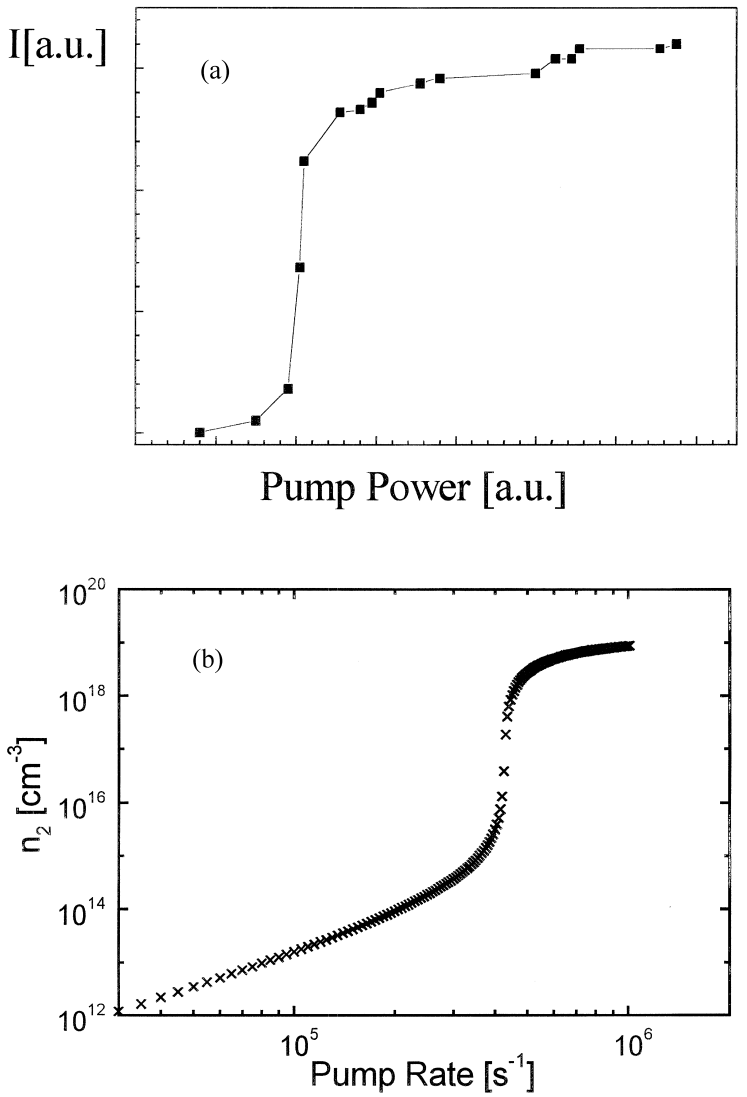

Fig. 6. a) Measured pump power dependence of the Pr^{3+} ($^3P_0$)→Pr^{3+} ($^3F_2$) emission in Pr,Yb:YLF, b) Pump power dependence of the Pr^{3+} (^3P_j) population in Pr,Yb:YLF derived from the rate equation model.

$$\frac{dn_1}{dt} = W_{YbPr} \cdot n_4 \cdot (N_{Pr} - n_1 - n_2) + W_{PrYb} \cdot (N_{Yb} - n_4) \cdot n_2 - W_p \cdot n_1 - W_1 \cdot n_1 + 2 \cdot W_{PrPr} \cdot (N_{Pr} - n_1 - n_2) \cdot n_2$$

$$\frac{dn_2}{dt} = W_p \cdot n_1 - W_2 \cdot n_2 - W_{PrYb} \cdot (N_{Yb} - n_4) \cdot n_2 - W_{PrPr} \cdot (N_{Pr} - n_1 - n_2) \cdot n_2$$

$$\frac{dn_4}{dt} = e \cdot W_p \cdot (N_{Yb} - n_4) - W_4 \cdot n_4 + W_{PrYb} \cdot (N_{Yb} - n_4) \cdot n_2 - W_{YbPr} \cdot n_4 \cdot (N_{Pr} - n_1 - n_2) -$$

$$N_{Pr} = n_0 + n_1 + n_2; \quad N_{Yb} = n_3 + n_4$$

Here, N_{Pr} (N_{Yb}) is the total Praseodymium (Ytterbium) concentration; n_0, n_1, and n_2 are population densities of the Pr energy levels $^3H_4$, $^1G_4$, and $^3P_{j=0,1,2}$, respectively, n_3, n_4 are the population densities of the Yb energy levels $^2F_{7/2}$ and $^2F_{5/2}$, respectively; W_p is the pump rate of the Pr $^1G_4 \rightarrow {}^3P_{j=0,1,2}$ transition, $e \cdot W_p$ is the pump rate of the Yb $^2F_{7/2} \rightarrow {}^2F_{5/2}$ transition with $e \approx 1 \times 10^{-6} - 1 \times 10^{-8}$ (for the meaning of e see below); W_{PrYb} is the transfer rate of process (2b); W_{YbPr} is the transfer rate of process (3); W_{PrPr} is the transfer rate of process (2a); W_1, W_2, and W_4 are the decay rates from the $^1G_4$, ^3P_j, and $^2F_{5/2}$ levels, respectively. The decay from the $^3P_{j=0,1,2}$ level into the $^1G_4$ level can be neglected. For modeling, data from spectroscopical results were used, as listed in Table 1.

For the pump power dependence of the emission, and therefore of the population in the $^3P_{j=0,1,2}$ level, steady state conditions were used. For YLF, the comparison between rate equation model and experiment is shown in Fig. 6a and b. The measured and calculated time depen-

Table 1
Crystals and parameters used for the rate equation model

	YLF	$YAlO_3$
N_{Pr} [10^{18} cm^{-3}]	24	120
N_{Yb} [10^{18} cm^{-3}]	763	890
$W_{PrPr}\times N_{Pr}$ [Hz]	4350	20 840
$W_{PrYb}\times N_{Yb}$ [Hz]	42 850	321 400
$W_{YbPr}\times N_{Pr}$ [Hz]	2840	17 500
W_1 [Hz]	90 900	250 000
W_2 [Hz]	20 000	83 000
W_4 [Hz]	500	1540

dencies are shown in Fig. 7a and b. The agreement between the calculation and the experimental results of the rise time of the red luminescence in Pr,Yb:YLF is satisfactory. The fast increase of the red luminescence measured for Pr,Yb:$YAlO_3$ is also reproduced.

Although both, the time dependence as well as the steady state behavior of the avalanche process is in general understood in the Yb–Pr systems, there are still open questions. First of all, the mechanism which provides the initial population in the $^1G_4$ is not known. In the rate equation model this problem was solved with the assumption, that somehow a small fraction of the pump power is absorbed by the Yb ion and transferred to the Pr $^1G_4$ level, although the pump wavelength is far from the Yb ground state absorption resonance. In principle, only a very low population in the Pr $^1G_4$ level is necessary to start the avalanche process, so that a vibrational sideband of the Yb $^2F_{7/2}\rightarrow{}^2F_{5/2}$ could be sufficient.

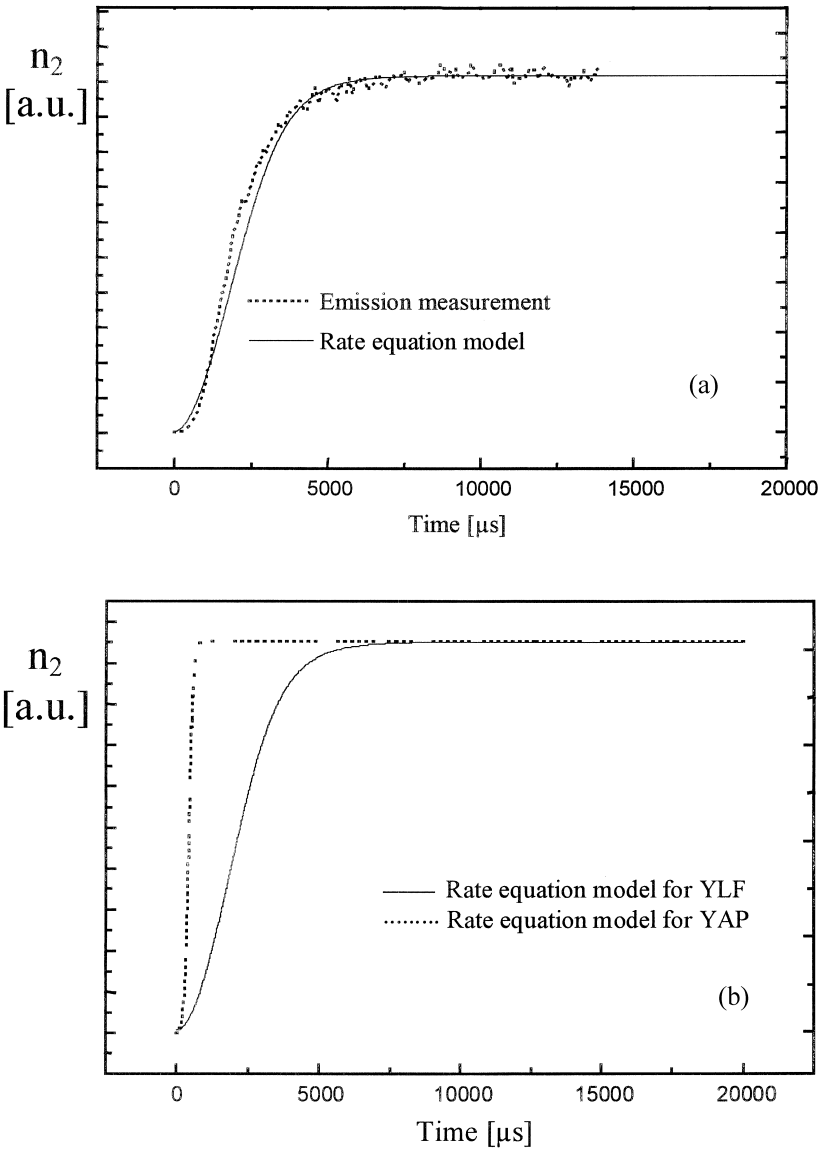

Fig. 7. (a) Temporal behavior of the Pr^{3+} (^3P_j) population in Pr,Yb:YLF, measured and derived from the rate equation model, (b) Comparison of the temporal behavior of the Pr^{3+} (^3P_j) population in Pr,Yb:YLF and Pr,Yb:$YAlO_3$ derived from the rate equation model.

5. Summary

In this contribution, the general characteristics of the 'Photon-Avalanche-Process' were presented. In particular, the spectroscopic behavior of the Yb–Pr systems was investigated in Pr,Yb:YLF and Pr,Yb:$YAlO_3$. The temporal behavior and the pump power dependence for the visible luminescence in Pr,Yb:YLF and Pr,Yb:$YAlO_3$ were presented and discussed. Whereas Pr,Yb:YLF shows an avalanche-type excitation process, Pr,Yb:$YAlO_3$ exhibits a two step excitation process via excited state and ground state absorption. A steady state and a time dependent rate equation model was developed, which in general reproduces the observed spectroscopic results. The main difference in the excitation behavior between the Yb–Pr system in YLF and $YAlO_3$ is caused by a stronger overlap between the Yb ground state absorption and Pr excited state absorption in $YAlO_3$, in the different decay rates of the participating energy levels and in a significant difference in the transfer rates W_{PrPr}, W_{PrYb}, and W_{YbPr}. Although a variety of spectroscopical data are presently available, it is still not completely understood, which parameter/process determines mainly the efficiency of the observed avalanche process. Furthermore the mechanism which provides the starting population in the $^1G_4$ level is still not known and needs further investigation.

References

[1] T. Sandrock, E. Heumann, G. Huber, B.H.T. Chai, in: S.A. Payne, C.R. Pollock (Eds.), OSA Trends in Optics and Photonics on Advanced Solid State Lasers, Vol. 1, Optical Society of America, Washington, DC, 1996, pp. 550–553.
[2] J.M. Sutherland, P.M.W. French, J.R. Taylor, B.H.T. Chai, in: S.A. Payne, C.R. Pollock (Eds.), OSA Trends in Optics and Photonics on Advanced Solid State Lasers, Vol. 1, Optical Society of America, Washington, DC, 1996, pp. 277–279.
[3] T. Sandrock, T. Danger, E. Heumann, G. Huber, B.H.T. Chai, Appl. Phys. B58 (1994) 149.
[4] E. Heumann, C. Czeranowsky, T. Kellner, G. Huber, in: Conference on Lasers and Electro-Optics, OSA Technical Digest, Paper CTuG1, Optical Society of America, Washington, DC, 1999.
[5] R. Scheps, Progress Quantum Electron. 20 (1996) 271.
[6] F. Auzel, Acta Phys. Polonica A 90 (1996) 7.
[7] F. Pellé, P. Goldner, Acta Phys. Polonica A 90 (1996) 197.
[8] M.-F. Joubert, Opt. Mater. 11 (1999) 181.
[9] S. Kueck, A. Diening, E. Heumann, E. Mix, K. Sebald, G. Huber, in: Advanced Solid State Lasers, OSA Technical Digest, Optical Society of America, Washington, DC, 1998, pp. 341–343.